Influence of electrochemical advanced oxidation on the long-term operation of an Upflow Anaerobic Sludge Blanket (UASB) reactor treating 4-chlorophenol containing wastewater

Jonas De Coster [1], Jia Liu [2], Rob Van den Broeck [1], Barbara Rossi [3,4], Raf Dewil [1,*], Lise Appels [1,*]

[1] *KU Leuven, Department of Chemical Engineering, Process and Environmental Technology Lab, J. De Nayerlaan 5, B-2860 Sint-Katelijne-Waver, Belgium*

[2] *Beijing University of Chemical Technology, Beijing Advanced Centre for Soft Matter Science and Engineering, 100029 Beijing, China*

[3] *KU Leuven, Department of Civil Engineering, Materials and Structures, J. De Nayerlaan 5, 2860 Sint-Katelijne-Waver, Belgium*

[4] *University of Oxford, Department of Engineering Science, Parks Road, Oxford OX1 3PJ, United Kingdom*

[*] *corresponding authors:*

raf.dewil@kuleuven.be *(R. Dewil)*, lise.appels@kuleuven.be *(L. Appels)*

Abstract

Upflow anaerobic sludge blanket (UASB) systems are of specific interest for the treatment of high organic wastewater since they offer the opportunity to recover energy in the form of methane (biogas). The technology is highly suitable for the degradation of biodegradable organics, but its efficiency can be significantly hampered by the presence of toxic pollutants in the water. In this study, the use of electrochemical advanced oxidation (eAOP) coupled to a lab-scale UASB reactor for the degradation of 4-chlorophenol (4-CP) in wastewater was investigated. The eAOP treatment consisted of the electrochemical production of active chlorine at a Ti/RuO_2-IrO_2 anode with a fixed current density of 25 mA/cm^2 in the recycle of the UASB reactor. It was noticed that the total COD removal efficiency decreased from 75.8% when no 4-CP was present in the wastewater to 25.6% and 13.6% after the addition of 100 ppm and 50 ppm 4-CP, respectively. Furthermore, elevated levels of volatile fatty acids and ORP were observed in the effluent of the reactor, indicating process failure. It was postulated that the decrease in COD removal efficiency was due to the release of high amounts of hypochlorite, causing an oxidative environment in the anaerobic reactor. This hypochlorite may have reacted with several components such as ammonia to form other toxic components (e.g., chloramine).

Keywords: anaerobic wastewater treatment; UASB; chlorophenol; inhibition; biogas

1. Introduction

Anaerobic treatment is a very attractive technique for the purification of wastewater that is heavily loaded with organic matter and contains a limited amount of nutrients (van Lier et al., 2008). The recovery of energy in the form of methane (biogas) is a specific benefit of the technology. Both municipal and industrial wastewater can be anaerobically treated, the latter originating from various sectors including food, pharmaceutical and the pulp and paper industry (Atashi et al., 2010; Ghangrekar et al., 2005; MacArie, 2000). The high purification efficiency, low sludge production, high-energetic biogas generation and simplicity in reactor design and operation are only a few benefits of anaerobic treatments (Bhatti et al., 2014). One of the most frequently applied reactor configurations is the Upflow Anaerobic Sludge Blanket reactor (UASB). This high rate reactor is able to efficiently treat high chemical oxygen demand (COD) loaded wastewater in short hydraulic retention times (HRT) (Yasar and Tabinda, 2010). Various papers have already assessed the biogas production from a UASB in different configurations, including co-digestion of wastewater with another organic waste or side stream (Chan et al., 2018) and the combination of different treatment techniques (Taki et al., 2019). Rosa et al. (2018) included both biogas production and the sludge generated in the process to determine the energy potential of an UASB treatment system. Modelling efforts were done by e.g., Lohani et al. (2016), who calibrated and validated the ADM1 model towards its use for UASB systems. In addition, hydrogen gas production was assessed in Ning et al., 2013.

The types of wastewater treated in a UASB vary considerably in composition (Ersahin et al., 2011) and the presence of toxic or inhibitory components may cause instability of the anaerobic reactor (Vidal et al., 1999). One specific group of highly toxic components are chlorinated aromatics such as chlorophenols which are for example originating from

64 cellulose pulp plants (Buzzini et al., 2005). The literature reveals that the anaerobic
65 metabolism is capable of degrading chlorophenols through reductive dechlorination but
66 only low concentrations are metabolized (Ye and Shen, 2004). Buzzini et al. (2005) added
67 a mix of chlorophenols to a UASB reactor in slowly increasing concentration up to 15
68 ppm and achieved effective degradation. Majumder and Gupta (2008) required a 230 day
69 adaptation period for a UASB reactor loaded with 40 ppm of 4-chlorophenol (4-CP). Such
70 large stabilization periods are not acceptable in full scale installations. Higher
71 chlorophenol concentrations unavoidably lead to reactor failure, if no additional treatment
72 is present to support their removal (Katsoni et al., 2014a; Majumder and Gupta, 2008;
73 Yasar and Tabinda, 2010). Additionally, due to an incomplete degradation, residual
74 chlorophenol concentrations would be present in the effluent.

75 Several authors such as Katsoni et al. (2014b) and Yasar and Tabinda (2010) have already
76 suggested the use of (electrochemical) advanced oxidation processes (eAOP) in
77 combination with an UASB reactor. The oxidation process is often used as effluent
78 polishing step for the removal of residual COD, color and pathogens from the UASB
79 effluent (Dewil et al., 2017). This approach, however, does not decrease the concentration
80 of recalcitrant or toxic components in the UASB itself.

81 In this work, an eAOP is applied in the recycle feed of a continuously operating UASB
82 to remove 4-CP from the recycled wastewater and hence lower its concentration in the
83 UASB reactor. A recycle process lay-out was chosen over an eAOP pre-treatment because
84 of the high concentration of biodegradable organic material in the influent, which would
85 consume a large fraction of the oxidation capacity of the eAOP, hence lowering its
86 efficiency towards 4-CP degradation. A commercially available Ti/RuO_2-IrO_2 anode was
87 used for the electrochemical treatment. Due to the presence of chloride ions in the

wastewater, an indirect oxidation is possible (i.e., oxidation by chloride as a mediator, which is electrochemically converted to active chlorine). The Ti/RuO_2-IrO_2 anode is well known to resist a chloride environment. The indirect oxidation pathway with active chlorine as oxidizing agent, on the removal of 4-CP, is therefore investigated.

2. Material and Methods

2.1. Synthetic wastewater and inoculum characteristics

A complex artificial wastewater containing macro- and micronutrients, was used to feed the continuous anaerobic reactor. The composition of wastewater was based on the artificial wastewater used by Ersahin et al. (2014). Its composition is listed in Table 1.

Granular anaerobic sludge, originating from a full-scale UASB process treating brewery wastewater (Duvel Moortgat, Belgium) was used as inoculum for the start-up of the lab-scale UASB reactor. This inoculum had a dry solid content (DS) of 44.8±0.8 g/L and an organic dry solid content (ODS) of 40.4±0.7 g/L.

2.2. Experimental set-up

A schematic representation of the experimental lay-out is depicted in Figure 1. A glass lab-scale UASB reactor (0.82 m in height) with a volume of 7.3 L, was used. At the top of the reactor, a 3-phase separator was installed to separate the biogas from the wastewater and the sludge granules. Sampling points in the headspace of the reactor enabled to take samples to analyze the composition of the biogas at regular time intervals. A water trap at the overflow of the reactor prevented biogas to escape with the effluent.

A 1 L glass electrochemical reactor was operated in a continuously mixed mode and was placed in the recycle over the UASB reactor. The electrochemical reactor was equipped with a water jacket for temperature control. The solution was constantly magnetically

111 stirred and the level remained constant due to the use of a level control. Parallel plate
112 electrodes (Ti cathode and Ti/RuO2-IrO2 anode) were placed inside the reactor. Each
113 electrode had an active surface area of 32 cm^2 (8x4 cm) and they were fixed at a constant
114 inter-electrode distance of 1 cm using polyamide screws. A constant current
115 (galvanostatic conditions) was applied using a lab scale power supply (Elektro Automatik
116 EA-PSI 8160-04 DT). $CaCl_2$ was used as supporting electrolyte at a concentration of ±1.5
117 g/L (i.e., ±1 g/L of Cl^-) because of the ability of Ca^{2+} to enhance the granulation process
118 of the microorganisms (Boonsawang et al., 2008).

119 To start up the UASB, 30% of the reactor volume (2.4 L) was filled with granular sludge.
120 Then the artificial wastewater (stock solution was diluted to attain a COD concentration
121 of ±1000 mg/L) was introduced at the bottom of the reactor at a constant volumetric flow
122 rate of 900 mL/min. This created an upflow velocity of 0.11 m/h (the cross sectional area
123 of the reactor was 0.785 dm^2). Therefore, the organic loading (OLR) was ±3 kg
124 COD/(m^3.d). When the recycle stream over the CSTR reactor was switched on, this
125 volume was not adapted, leading to a double effective upflow velocity in the UASB
126 (recycle ratio of 1/1 v/v).

127 The artificial wastewater was kept in a cooled buffer tank, which was constantly mixed
128 by a mechanical stirrer at 100 RPM. The water was pumped in the UASB reactor at the
129 preset flow rate by a peristaltic pump (Verderflex BEZ 3000). The same type of pump
130 was used to recycle part of the effluent over the electrochemical reactor.

131 **2.3. Analytical techniques**

132 The pH and an Oxidation Reduction Potential (ORP) were continuously monitored in the
133 sludge bed of the UASB reactor using a PHC10101 and MTC10101 sensor, respectively,

connected to a HQ40d portable meter (Hach, Belgium). These sensors also included an integrated temperature measurement. The COD of the influent and effluent were analyzed using a closed reflux colorimetric method (Method 5220D, APHA) with Hach test tubes and a DR3900 Benchtop Spectrophotometer (Greenberg et al., 1992). pH (PHC10101 sensor - Hach, Belgium) and conductivity (CDC10101 sensor - Hach, Belgium) were also manually measured in the influent and effluent of the reactor. Analysis of VFA in the reactor effluent was performed using a GC-FID (Agilent 7890A) with a HP-FFAP Innowax column (30mx0.25mmx0.25µm). A volume of 500 µL of each sample was acidified with H_2SO_4 in the presence of NaCl and an internal standard (i.e., 2-methylvaleric acid). Then, the VFA were extracted on ice using diethyl ether. The water and the organic phase were separated via centrifugation and the latter was collected for injection. A volume of 1µL of the organic phase was injected in the GC-FID. The FID was operated at a constant temperature of 240°C and the flame was created by the use of H_2 and air. Helium was used as a carrier gas. The inlet temperature was 200°C and the oven temperature profile was varied from 45°C (1 min) to 200°C (4.5 min) with a rate of 10°C/min. The system was calibrated for acetic acid, propionic acid, isobutyric acid, butyric acid, isovaleric acid, caproic acid and levulinic acid.

The biogas production was continuously measured by a calibrated drum-type gas meter (Ritter TG05, model 5). Biogas quality was determined using a GC-TCD (Hewlett Packard G1540A) with manual injection of 500 µL in split mode. The TCD-detector was maintained at a constant temperature of 250°C with helium as reference gas. The used column (Agilent Poraplot U with 2 particle traps, 25 m x 0.53 mm x 20 µm) was heated for 3.5 min at 80°C.

157 The concentration of 4-CP and the main intermediates in the eAOP process, i.e., 2,4-
158 dichlorophenol (2,4-DCP) and 2,4,6-trichlorophenol (2,4,6-TCP), were measured using
159 an HPLC (Agilent 1100 Series), equipped with a reversed-phase C18 column (Agilent,
160 Zorbax Eclipse Plus C18 4.6 x 100 mm; 3.5 µm) and a UV detector (280 nm). The mobile
161 phase was a mixture of methanol and water (40/60) and the injection volume was 3 µL.

162 To determine residual hypochlorite, a standard iodometric titration was performed. A
163 sample volume of 5 mL was acidified with 20 mL of H_2SO_4 (1M) and 25 mL of KI
164 (0.2M) was added. A few drops of starch (1%) were added as indicator. The solution
165 was then titrated with $Na_2S_2O_3$ (0.05M).

166 **2.4. Residence Time Distribution (RTD)**

167 Theoretically, the residence time of all fluid elements (RT) in a reactor that is operated in
168 ideal plug flow equals the volume of the reactor divided by the flow rate. Plug flow is
169 indeed considered ideal, since all flow elements have an equal average residence time,
170 thus leading to an equal conversion when exiting the reactor. On the contrary, fluid
171 elements have a wide range of residence times in a Continuous Stirred Tank Reactor
172 (CSTR), leading to a wide spread of conversions. Similar treatments have already been
173 reported for various gas/solid/liquid processes (Deng et al., 2019; Kong et al., 2018;
174 Mahmoudi et al., 2011; Chan et al., 2009; Van de Velden et al., 2007). In the case of the
175 UASB reactor applied in the experiments, the RT would be 7.3 L / (0.9 L/h), equaling 8.1
176 h. However, due to non-ideal fluid flow through the reactor, a residence time distribution
177 (RTD) will occur, which was determined based on tracer pulse injection tests. In this test,
178 the UASB reactor was fed with demineralized water (constant flowrate of 1.2 L/h) and
179 the conductivity of the effluent was measured. After a baseline in conductivity was
180 achieved, a pulse containing a concentrated salt solution (2 g NaCl in 10 mL

demineralized water) was injected into the reactor's feeding tube. The mean residence time was then calculated based on the conductivity profile of the effluent. First, the residence time distribution E(t) at each time is calculated, (1) (Levenspiel, 1999):

$$E(t) = \frac{\sigma}{\int \sigma dt} \quad (1)$$

With E(t) the residence time or exit age distribution, σ the conductivity (µS/cm) and t the time (s).

After calculating this value for each data point, the mean RT is calculated by summation of all values for the integral of t E(t) with time, (2).

$$\text{Mean RT} = \sum_{i=1}^{n} \int tE(t)dt \quad (2)$$

The simple tracer pulse response method provides a good approximation of the RTD (Deng et al., 2019; Kong et al., 2018; Mahmoudi et al., 2011; Chan et al., 2009; Van de Velden et al., 2007). The production of biogas and the presence of granular sludge in an UASB reactor in operation result in higher mixing, which would require much more complex RTD models for full evaluation, however beyond the scope of this research.

3. Results and discussion

3.1. Residence Time Distribution (RTD)

Figure 2A shows the profile for the RTD, calculated with (1) and (2), in the lab-scale UASB reactor based on the pulse test with NaCl. The tracer pulse was measured and injected at time 0. Also, a theoretical RTD distribution model was plotted in the figure, which corresponds to an ideal CSTR placed in series with a PFR. The model equation is added in (3) (Levenspiel, 1999).

$$E(t) = \frac{v}{V_M} \exp\left[-\frac{v}{V_M}t + \frac{V_P}{V_M}\right] \quad (3)$$

With E(t) the residence time distribution (RTD) (1/s), t the time (s), v the flowrate (m^3/s), V_M the volume of the ideal CSTR (m^3), and V_P the volume of the ideal PFR (m^3).

All parameters in this equation are defined since the flowrate v is fixed at 1.2 L/h, and since Levenspiel (1999) described the v/V_M parameter as the maximal calculated value of E(t) resulting from the data points. This maximum is reached after a time V_P/v. The other parameter is calculated by dividing the values of the first two ones. After calculating these parameters, the model was plotted (Figure 2A) and it was seen that it fitted the data points quite accurately.

Also resulting from the model parameter values, V_P/V_M was determined to be 0.44. This implies that the reactor can be compared to a an ideal PFR and CSTR in series, by which the theoretical volume of the PFR is 44% of the combined reactor volume.

Based on the experimental data points and (2), the mean RT for the reactor was calculated to be 14.9 h, whereas the suggested model predicted a mean RT of 14.1 h, which is close to the experimental one. Based on the model, 90% of the fluid elements passing through the reactor had an RTD lower than 13.6 h.

In a second experiment, the effect of the presence of a CSTR in recycle over the UASB reactor on the RTD was evaluated. The same procedure was carried out as before, giving the result as shown in Figure 2B. The experimental mean RT was 9.8 h in this case, whereas the model suggested 12.7 h for 90% of the fluid passing through the reactor. This is lower than the 13.6h for the case of the UASB reactor only. This lower value is contradictory because adding the recycle will increase the total liquid flow rate through the same reactor volume and it will hence decrease the RT. This can however be explained by the fact that the model for the UASB with recycle underestimates the experimental

values, as can also be seen from Figure 1B. The percentage of PFR and CSTR behavior was 12% and 88%, respectively, which is logical due to the addition of a CSTR in recycle. Another observation in this RTD is the slight increase in E(t) for the first 300 minutes after dosing the NaCl pulse. This may indicate the presence of a short-circuiting flow.

3.2. Start-up and stabilization of the UASB reactor

After the inoculum was added to the UASB reactor, the synthetic wastewater was continuously fed for 72 days in order to guarantee that the anaerobic bacteria were adapted to the artificial wastewater. Several process parameters (pH, T and ORP inside the reactor, COD, VFA, pH and conductivity of the effluent and biogas production) were followed during this stabilization period. Figure 3 illustrates the ORP, pH and T inside the reactor. Throughout the adaptation, these values remained at a nearly constant value and were all in range of stable UASB operation. For anaerobic reactors, the ORP should be lower than -200 mV (Appels et al., 2008; Moletta, 2005). pH should generally be between 6.5 and 8. Mesophilic conditions require temperatures in the range of 30-38°C (Appels et al., 2008). The ORP value was observed to be systematically below -400 mV indicating anaerobic stability (apart from the few peak values, which were due to the recalibration of the sensors placed in the UASB). This low value is explained by the biological reduction to sulfide of the sulfate, present in the artificial wastewater, which takes place in the range around -400 mV (Zhang et al., 2014). The average pH in the sludge bed was 7.78. The temperature inside the reactor was kept constant at 33.3 °C, corresponding to mesophilic conditions.

Figure 4 shows the removal of the total and soluble fraction of the wastewater COD. Over the 72 days stabilization period, the average total COD of the influent was 889 mg O_2/L and the total COD of the effluent was 215.4 mg O_2/L. This resulted in an average removal

250 efficiency of 75.8%. For the soluble fraction of the COD, the average removal ratio was
251 85.4%. The removal rates of both parameters remained at the same level throughout the
252 stabilization period. The biogas production showed some daily fluctuations, but on
253 average it was 4.1 L/d. The methane (CH_4) concentration of the produced biogas was on
254 average 67.8%. For the observed COD degradation, the maximal theoretical biogas
255 production is ± 8.7 L/d (Metcalf and Eddy, 2003), meaning that only 47% of the produced
256 biogas was recovered. This considerable difference is attributed to dissolution of the
257 biogas in the effluent water, which is frequently encountered for small-scale lab systems
258 as was also observed by other authors (Aiyuk and Verstraete, 2004; Crone et al., 2016).
259 No residual VFA were found in the UASB effluent, indicating a stable operation and good
260 methanogenic activity.

261 **3.3. Operation at 1/1 recycle ratio**

262 During the second experimental period, a recycle stream (1/1 v/v) was applied to the
263 UASB reactor implying that (in regime) half of the effluent was recycled into the reactor.
264 The results for the total and soluble COD removal are depicted in Figure 5. Throughout
265 this period, the average removal efficiency for the total and soluble COD were 85.6% and
266 87.7%, respectively. This is an increase by 9.8% and 2.3% compared to the first
267 experimental period during which the UASB was operated without recycle. The increase
268 in COD removal efficiency is in accordance with previous results obtained by Ladu and
269 Lü (2014), which also reported an increase in COD removal efficiency when applying a
270 recycle.

271 ORP, pH and temperature were not significantly different compared to the first
272 experimental period. Their average values were -433.3mV, 7.14 and 33.1°C, respectively.

273 The average daily biogas production was 4.2 L/d (containing 67% methane on average)
274 and again, no VFA were found in the effluent.

275 **3.4. Electrochemical treatment of 4-CP in recycle**

276 The presence of 4-chlorophenol (4-CP) in the influent may cause inhibition of the
277 anaerobic micro-organisms already at relatively low concentration, causing a lower COD
278 removal efficiency and lower biogas production. Puyol et al. (2012) reported EC50 values
279 for 4-CP that vary between 26 and 300 ppm, depending on several factors such as the
280 type of anaerobic reactor, sludge characteristics and the sludge's pre-exposure to some
281 toxic components. Especially methanogens are prone to inhibition although in most cases
282 a reversible inhibition occurs (Vidal et al., 1999).

283 During the third experimental period, 4-CP was added to the artificial wastewater fed to
284 the UASB reactor at a concentration of 100 ppm. The eAOP treatment was applied on
285 the recycle (applied current density J of 25 mA/cm^2), as depicted in Figure 1.

286 During the first phase of the experiment, the total COD removal decreased to 25.6%
287 during electrochemical treatment, cfr. section I in Figure 5. Furthermore, VFA
288 concentrations increased, with an average value of 151 ppm in the effluent, indicating
289 failure of the reactor. The average pH value of the effluent during treatment was 7.4. For
290 these reasons, it was decided after 10 days to temporarily stop the addition of 4-CP to the
291 influent as well as the eAOP treatment to avoid failure of the reactor. Subsequently, the
292 reactor was left to stabilize during a period of 20 days (cfr. section II in Figure 5). During
293 this period, a revival of the reactor's activity was observed, witnessed by an increase in
294 total and soluble COD removal to 80.4% and 70.4%, respectively, indicating that the
295 anaerobic bacteria were capable of recovering relatively fast in a stable environment. In

296 the third phase of the experiment, the dosage of 4-CP in the wastewater was reduced to
297 50 ppm, and the same eAOP treatment (i.e., current density J of 25 mA/cm²) was applied
298 (cfr. section III in Figure 5). However, after 10 days, the total and soluble COD removal
299 decreased to 13.6% and 27.9% respectively. Although the pH remained stable at an
300 average value of 7.4, VFA concentrations of 242 ppm on average were found in the
301 effluent, meaning that the reactor was destabilized by the addition of 50 ppm 4-CP and
302 was not able to effectively degrade the phenol.

303 After a second successful stabilization period (i.e., section IV), a final eAOP treatment
304 was applied on the recycle stream (i.e., section V) without the addition of 4-CP in the
305 influent wastewater. With this experiment, the effect of the electrochemically produced
306 hypochlorite on the anaerobic microorganisms could be investigated. A decrease in total
307 and soluble COD removal to 37% and 30% respectively was observed, indicating the
308 negative effect of the eAOP. However, contrarily to the results of phase I and III, no
309 residual VFA were found in the effluent. These results indicate that although COD
310 removal is reduced, the level of inhibition due to the application of eAOP solely is lower
311 than in the presence of 4-CP.

312 Figure 6 shows the results for the ORP, pH and temperature measurements in the reactor
313 during the whole experimental run. It is clear that both pH and temperature remained
314 relatively stable throughout the different phases, except for the drop in temperature during
315 phase I, due to a power failure in the lab. During the phases corresponding to the addition
316 of 4-CP combined with eAOP treatment (i.e., I and III in Figure 6), a clear increase in
317 ORP was shown. This increase, up to -20 mV for phase I and up to +340 mV in phase III,
318 is most probably due to the production of hypochlorite in the recycle reactor. Excess
319 amounts of this oxidizing agent may possibly be re-introduced into the UASB reactor,

causing oxidation reactions in the reactor and therefore an increase in ORP. In section V, a larger increase in ORP value was observed, up to +880 mV. This difference in maximal ORP value for these three successive phases is attributed to the decrease in 4-CP concentration, which reacts with the oxidizing agent, from 100, 50 to 0 ppm.

Another explanation for this failure could also be attributed to the formation of intermediate components during the electrochemical oxidation. Despite the fact that previous batch experiments showed that the toxicity of 4-CP decreased if an eAOP treatment was carried out under controlled conditions, some problems could occur in the continuous scale experiments. Since the synthetic wastewater and the recycled effluent (which may contain excess hypochlorite) are both introduced at the bottom of the UASB near each other, hypochlorite may attack some components in the synthetic wastewater. In particular, hypochlorite can oxidize ammonia or ammonia-containing substrates. Reactions (4) and (5) show the possible reactions of hypochlorite with ammonia (NH_4^+) and urea ($(NH_2)_2CO$), leading to toxic intermediates such as chloramine (NH_2Cl), which can react with NH_3 (formed by oxidation of urea) to the toxic hydrazine (N_2H_4), reaction (6) (Lawrence, 2004). In a few cases, also toxic dichloramine ($NHCl_2$) and trichloramine (NCl_3) can be formed if chlorine is abundantly present, reactions (7) and (8) (The National Academies, 1980). Finally, also (toxic) organic chloramines may be formed.

$$ClO^- + NH_4^+ \rightarrow NH_2Cl + H_2O \quad (4)$$

$$3ClO^- + 2(NH_2)_2CO \rightarrow 2NH_3 + N_2 + H_2O + 3Cl^- \quad (5)$$

$$NH_2Cl + NH_3 \rightarrow N_2H_4 + HCl \quad (6)$$

$$ClO^- + NH_2Cl \rightarrow NHCl_2 + OH^- \quad (7)$$

$$ClO^- + NHCl_2 \rightarrow NCl_3 + OH^- \quad (8)$$

343 The use of hypochlorite as such for biocidal use is also widely studied. Because of the
344 strong affection of this chlorine containing component towards nitrogen, amino acids and
345 other proteins are easily chlorinated (European Commission, 2002). A report from the
346 European Commission indicated that very low concentrations of hypochlorite in water
347 (0.1 to 1 mg/L) already strongly inhibits bacterial growth due to the partial destruction of
348 the proteins in cell membranes (European Commission, 2002; Venkobachar et al., 1977).

349 The analysis of the presence of free hypochlorite revealed that during Phase I and III, an
350 average concentration of 18 ppm and 21 ppm was found in the effluent, respectively. In
351 the last eAOP phase, a concentration of 22 ppm was found in the effluent. Considering
352 the inhibition values for bacterial growth that were reported by the European Commission
353 (2002), such amounts of free hypochlorite in the reactor may affect bacterial growth and
354 activity. Furthermore, hypochlorite concentrations up to 33 ppm were found in the recycle
355 stream. The difference in this value, compared to the effluent concentrations (i.e., 18, 21
356 and 22 ppm), could be attributed to the reaction of hypochlorite with nitrogen-containing
357 components in the wastewater, as previously explained in this paragraph. It is therefore
358 recommended that, the effluent should be analyzed with HPLC-MS to elucidate the
359 formation of intermediary and secondary compounds, but this was however not included
360 in the scope of this study.

361 From the results described above, it is not conclusively proven that only the residual
362 hypochlorite causes toxicity. This excess hypochlorite causes increase in ORP and can
363 cause production of other toxic components such as hydrazine and chloramine, but it is
364 not ruled out that intermediary and secondary compounds formed during 4-CP
365 degradation do not have an adverse effect on the anaerobic process.

3.5. Energetic analysis of the eAOP treatment

In order to validate the energetic feasibility of the electrochemical oxidation treatment, the required voltage for maintaining the fixed current density of 25 mA/cm² was monitored during the experimental set-up. In the beginning, the required voltage was 6.5-7 V considering the applied current density and conductivity of the wastewater. The associated power consumption for these conditions was 5-5.5 W. Since the active volume in the eAOP reactor remained 1 L at all times, this power consumption implies a specific power consumption of 5.5 Wh/L or 5.5 kWh/m³. A comparison against values for other (electrochemical) advanced oxidation processes, as listed in Table 2, reveals that this value is rather low. This table is based on the results presented by Mahamuni and Adewuyi (2010) and Martínez-huitle and Andrade (2011), who degraded reactive azo-dyes. The table also represents the general feasibility of electrochemical oxidation processes, if a proper electro-catalytic anode is chosen, towards more traditional AOP.

Particulate matter, such as non-degraded insoluble organics and sludge granules, however tend to foul the cathode during operation. This fouling caused an increase in power consumption. After two days, the required voltage increased to 100 V, which was the maximum voltage that the power supply could provide. Therefore, the current density decreased to 18 mA/cm², affecting the reaction kinetics of 4-CP degradation and the specific energy consumption, which increased to 57 kWh/m³, i.e., more than a factor 10 times higher than the one at the beginning.

4. Conclusions

In this study, the use of electrochemical advanced oxidation (eAOP) coupled to a lab-scale UASB reactor for the degradation of 4-chlorophenol (4-CP) in wastewater was investigated. The eAOP treatment consisted of the electrochemical production of active

chlorine at a Ti/RuO_2-IrO_2 anode with a fixed current density of 25 mA/cm^2 in the recycle of the UASB reactor. It was noticed that the total COD removal efficiency decreased from 75.8% when no 4-CP was present in the wastewater to 25.6% and 13.6% after the addition of 100 ppm and 50 ppm 4-CP, respectively. Furthermore, elevated levels of volatile fatty acids and ORP were observed in the effluent of the reactor, indicating process failure. It was postulated that the decrease in COD removal efficiency was due to the release of high amounts of hypochlorite, causing an oxidative environment in the anaerobic reactor. This hypochlorite may have reacted with several components such as ammonia to form other toxic components (e.g., chloramine).

Acknowledgements

The authors would like to thank the Industrial Research Council of KU Leuven – Knowledge Platform AOPtimise (KP/10/006), and the Research Council of KU Leuven (OT/13/063) for the financial support.

References

Aiyuk, S., Verstraete, W., 2004. Sedimentological evolution in an UASB treating SYNTHES, a new representative synthetic sewage, at low loading rates. Bioresour. Technol. 93, 269–278. doi:10.1016/j.biortech.2003.11.006

Appels, L., Baeyens, J., Degrève, J., Dewil, R., 2008. Principles and potential of the anaerobic digestion of waste-activated sludge. Prog. Energy Combust. Sci. 34, 755–781. doi:10.1016/j.pecs.2008.06.002

Atashi, H., Ajemaine, H., Ghasemian, S., 2010. Effect of Operational and Design Parameters on Removal Efficiency of a Pilot-Scale UASB Reactor in a Sugar Factory. World Appl. Sci. J. 11, 451–456.

Bhatti, Z.A., Maqbool, F., Malik, A.H., Mehmood, Q., 2014. UASB reactor startup for the treatment of municipal wastewater followed by advanced oxidation process. Brazilian J. Chem. Eng. 31, 715–726. doi:10.1590/0104-6632.20140313s00002786

Boonsawang, P., Laeh, S., Intrasungkha, N., 2008. Enhancement of sludge granulation in anaerobic treatment of concentrated latex wastewater. Songklanakarin J. Sci. Technol. 30, 111–119.

Buzzini, A.P., Gianotti, E.P., Pires, E.C., 2005. UASB performance for bleached and unbleached kraft pulp synthetic wastewater treatment. Chemosphere 59, 55–61. doi:10.1016/j.chemosphere.2004.09.102

Chan, C.W., Seville, J., Fan, X., Baeyens, J, 2009. Solid particle motion in a standpipe as observed by Positron Emission Particle Tracking. Powder Technology 194, 58-66. Doi: 10.1016/j.powtec.2009.03.032

Chan, P.C., Alves de Toledo, R., Shim, H., 2018. Anaerobic co-digestion of food waste and domestic wastewater – Effect of intermittent feeding on short and long chain fatty acids accumulation. Ren. Energ. 124, 129-135. Doi: 10.1016/j.renene.2017.07.029

Crone, B.C., Garland, J.L., Sorial, G.A., Vane, L.M., 2016. Significance of dissolved methane in effluents of anaerobically treated low strength wastewater and potential for recovery as an energy product: A review. Water Res. 104, 520–531. doi:10.1016/j.watres.2016.08.019

Deng, Y., Ansart, R., Baeyens, J., Zhang, Y., 2019. Flue Gas Desulphurization in Circulating Fluidized Beds. Energies 12(20). Doi: 10.3390/en12203908

Dewil, R., Mantzavinos, D., Poulios, I., Rodrigo M.A., 2017. New perspectives for Advanced Oxidation Processes. J. Env. Manag. 195, 93-99. Doi: 10.1016/j.jenvman.2017.04.010

Ersahin, M.E., Ozgun, H., Dereli, R.K., Ozturk, I., 2011. Anaerobic treatment of industrial effluents: An overview of applications. Waste Water-treatment Reutil. 3–28.

Ersahin, M.E., Ozgun, H., Tao, Y., van Lier, J.B., 2014. Applicability of dynamic membrane technology in anaerobic membrane bioreactors. Water Res. 48, 420–429. doi:10.1016/j.watres.2013.09.054

European Commission, 2002. European Union Risk Assessment Report 5.

443 Ghangrekar, M.M., Asolekar, S.R., Joshi, S.G., 2005. Characteristics of sludge developed under
444 different loading conditions during UASB reactor start-up and granulation. Water Res. 39,
445 1123–1133. doi:10.1016/j.watres.2004.12.018

446 Greenberg, A.E., Clesceri, L.S., Eaton, A.D., 1992. Standard methods for the examination of
447 water and wastewater np.

448 Katsoni, A., Mantzavinos, D., Diamadopoulos, E., 2014a. Coupling digestion in a pilot-scale
449 UASB reactor and electrochemical oxidation over BDD anode to treat diluted cheese whey.
450 Environ. Sci. Pollut. Res. 12170–12181. doi:10.1007/s11356-014-2960-2

451 Katsoni, A., Mantzavinos, D., Diamadopoulos, E., 2014b. Sequential treatment of diluted olive
452 pomace leachate by digestion in a pilot scale UASB reactor and BDD electrochemical oxidation.
453 Water Res. 57, 76–86. doi:10.1016/j.watres.2014.03.010

454 Kong, W., Wang, B., Baeyens, J., Li, S., Ke, H., Tan, T.W., Zhang, H., 2018. Solids mixing in a
455 shallow cross-flow bubbling fluidized bed. Chem. Eng. Sci. 187, 213-222. Doi:
456 10.1016/j.ces.2018.04.073

457 Ladu, J.L.C., Lü, X., 2014. Effects of hydraulic retention time, temperature, and effluent
458 recycling on efficiency of anaerobic filter in treating rural domestic wastewater. Water Sci. Eng.
459 7, 168–182. doi:10.3882/j.issn.1674-2370.2014.02.005

460 Lawrence, S., 2004. Amines: synthetis, properties and applications. Cambridge University
461 Press, Cambridge.

462 Levenspiel, O., 1999. Chemical reaction engineering. Chem. Eng. Sci. doi:10.1016/0009-
463 2509(64)85017-X

464 Lohani, S.P., Wang, S., Lackner, S., Horn, H., Khanal, S.N., Bakke, R., 2016. ADM1 modeling of
465 UASB treating domestic wastewater in Nepal. Ren. Energ. 95, 263-268. doi:
466 10.1016/j.renene.2016.04.014

467 MacArie, H., 2000. Overview on the application of anaerobic digestion to the treatment of
468 chemical and petrochemical wastewaters. Inst. Rech. pour le Dévelopement 405–412.

469 Mahamuni, N.N., Adewuyi, Y.G., 2010. Advanced oxidation processes (AOPs) involving
470 ultrasound for waste water treatment: A review with emphasis on cost estimation. Ultrason.
471 Sonochem. 17, 990–1003. doi:10.1016/j.ultsonch.2009.09.005

472 Mahmoudi, S., Baeyens, J., Seville, J., 2011. The solids flow in the CFB-riser quantified by single
473 radioactive particle tracking. Powder Technology 211, 135-143. Doi:
474 10.1016/j.powtec.2011.04.011

475 Majumder, P.S., Gupta, S.K., 2008. Degradation of 4-chlorophenol in UASB reactor under
476 methanogenic conditions. Bioresour. Technol. 99, 4169–4177.
477 doi:10.1016/j.biortech.2007.08.062

478 Martínez-huitle, C., Andrade, L.S., 2011. ELECTROCATALYSIS IN WASTEWATER TREATMENT:
479 RECENT MECHANISM ADVANCES. Quim. Nov. 34, 850–858.

480 Metcalf, E., Eddy, H., 2003. Wastewater engineering: treatment and reuse. Tata McGraw-Hill
481 Publ. Co. Limited, 4th Ed. New Delhi, India. doi:10.1016/0309-1708(80)90067-6

Moletta, R., 2005. Winery and distillery wastewater treatment by anaerobic digestion. Water Sci. Technol. 51, 137–144.

Ning, Y.Y., Wang, S.F., Jin, D.W., Harada, H., Shi, X.Y., 2013. Formation of hydrogen-producing granules and microbial community analysis in a UASB reactor. Ren. Energ. 53, 12-17. Doi: 10.1016/j.renene.2012.10.051

Puyol, D., Sanz, J.L., Rodriguez, J.J., Mohedano, A.F., 2012. Inhibition of methanogenesis by chlorophenols: A kinetic approach. N. Biotechnol. 30, 51–61. doi:10.1016/j.nbt.2012.07.011

Rosa, A.P., Chernicharo, C.A.L., Lobato, L.C.S., Silva, R.V., Padilha, R.F., Borges, J.M., 2018. Assessing the potential of renewable energy sources (biogas and sludge) in a full-scale UASB-based treatment plant. Ren. Energ. 124, 21-26. Doi: 10.1016/j.renene.2017.09.025

Taki, K., Gogoi, A., Mazumder, P., Bhattacharya, S.S., Kumar, M., 2019. Efficacy of vermitechnology integration with Upflow Anaerobic Sludge Blanket (UASB) and activated sludge for metal stabilization: A compliance study on fractionation and biosorption. J. Env. Manag. 236, 603-612. Doi: 10.1016/j.jenvman.2019.01.006

Van de Velden, M., Baeyens, J., Dougan, B., McMurdo, A., 2007. Investigation of operational parameters for an industrial CFB combustor of coal, biomass and sludge. China Particuology 5, 247-254. Doi: 10.1016/j.cpart.2007.05.001

Van Lier, J.B., Mahmoud, N., Zeeman, G., 2008. Biological wastewater treatment: principles, modelling and design – Chapter 16: Anaerobic wastewater treatment,IWA Publishing ed., Biological WasteWater Treatment: Principles, Modelling and Design.

Venkobachar, C., Iyengar, L., Prabhakara Rao, A.V.S., 1977. Mechanism of disinfection: Effect of chlorine on cell membrane functions. Water Res. 11, 727–729. doi:10.1016/0043-1354(77)90114-2

Vidal, G., Jiang, Z.P., Omil, F., Thalasso, F., Mendez, R., Lema, J.M., 1999. Continuous anaerobic treatment of wastewaters containing formaldehyde and urea. Bioresour. Technol. 70, 283–291. doi:10.1016/S0960-8524(99)00031-0

Yasar, A., Tabinda, A.B., 2010. Anaerobic Treatment of Industrial Wastewater by UASB Reactor Integrated with Chemical Oxidation Processes ; an Overview 19, 1051–1061.

Ye, F.X., Shen, D.S., 2004. Acclimation of anaerobic sludge degrading chlorophenols and the biodegradation kinetics during acclimation period. Chemosphere 54, 1573–1580. doi:10.1016/j.chemosphere.2003.08.019

Zhang, J., Li, G.-B., Ma, J., 2003. Effects of chlorine content and position of chlorinated phenols on their oxidation kinetics by potassium permanganate. J. Environ. Sci. 15, 342–345.

517

518 *Table 1: Composition of artificial wastewater used in the experiments*

Macronutrients	**g/L**		**Micronutrients**	**g/L**	
Urea	0.15		$FeCl_3.4H_2O$	1	
NH_4Cl	0.028		$CoCl_2.6H_2O$	1	
CH_3COONa	0.19		$MnCl_2.4H_2O$	0.25	
$CaCl_2.2H_2O$	1.54		$CuCl_2.2H_2O$	0.015	
Milk powder	0.28		$ZnCl_2$	0.025	
$MgSO_4.7H_2O$	0.013		$NiCl_2.6H_2O$	0.025	
K_2HPO_4	0.11		$(NH_4)_6Mo_7O_{24}.4H_2O$	0.045	
KH_2PO_4	0.086		$Na_2SeO_3.5H_2O$	0.05	
Ovalbumin	0.042		H_3BO_3	0.025	
Starch	0.3		EDTA	0.5	
Yeast extract	0.125		HCl (37%)	0.5	mL/L
Sunflower oil	0.07	mL/L	Resazurin	0.25	
Micronutrients	0.05	mL/L			

519

520 *Table 2: Specific energy consumption for different advanced oxidation processes*

	Anode	Specific energy consumption
Electrochemical oxidation	Pt	44,1
	PbO_2	1,86
	Ti/BDD	13,4
	O_3 (12,4	30
	O_3/UV	60
AOP	H_2O_2/UV	27

521

522

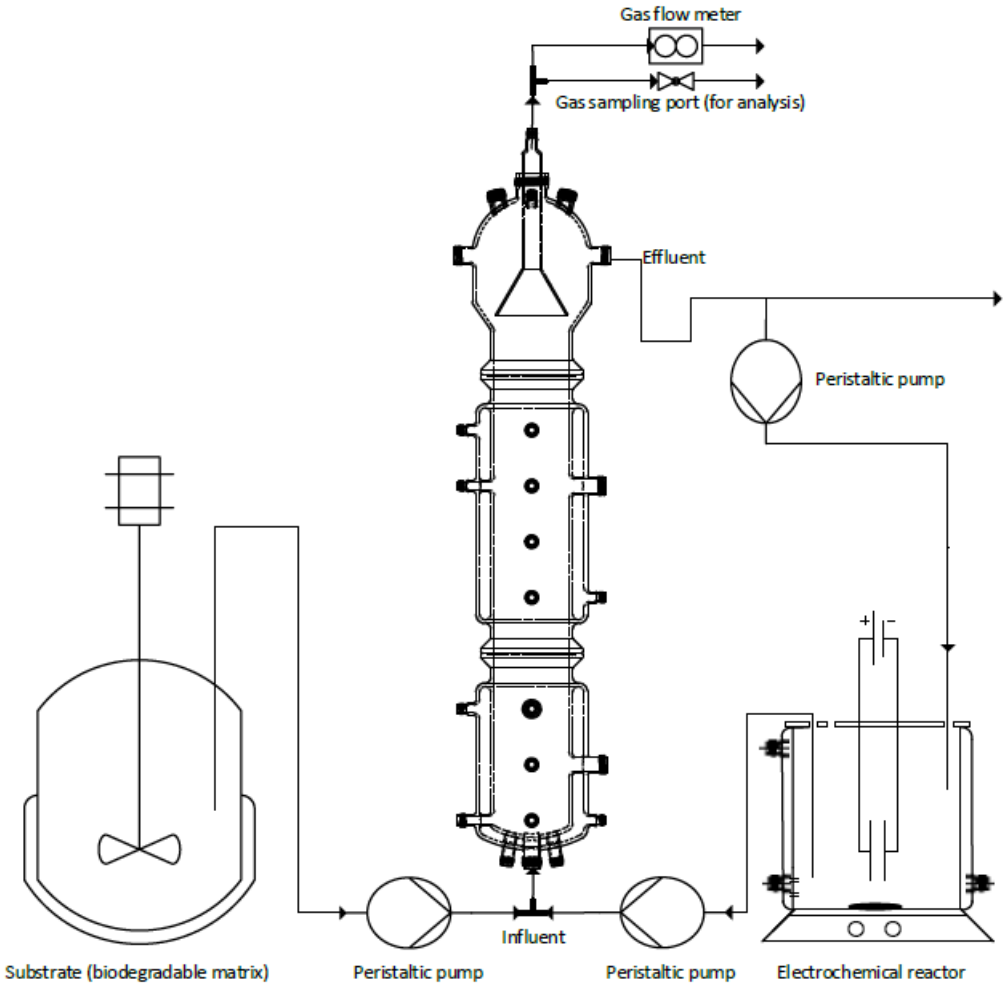

523

524 *Figure 1: Experimental lay-out*

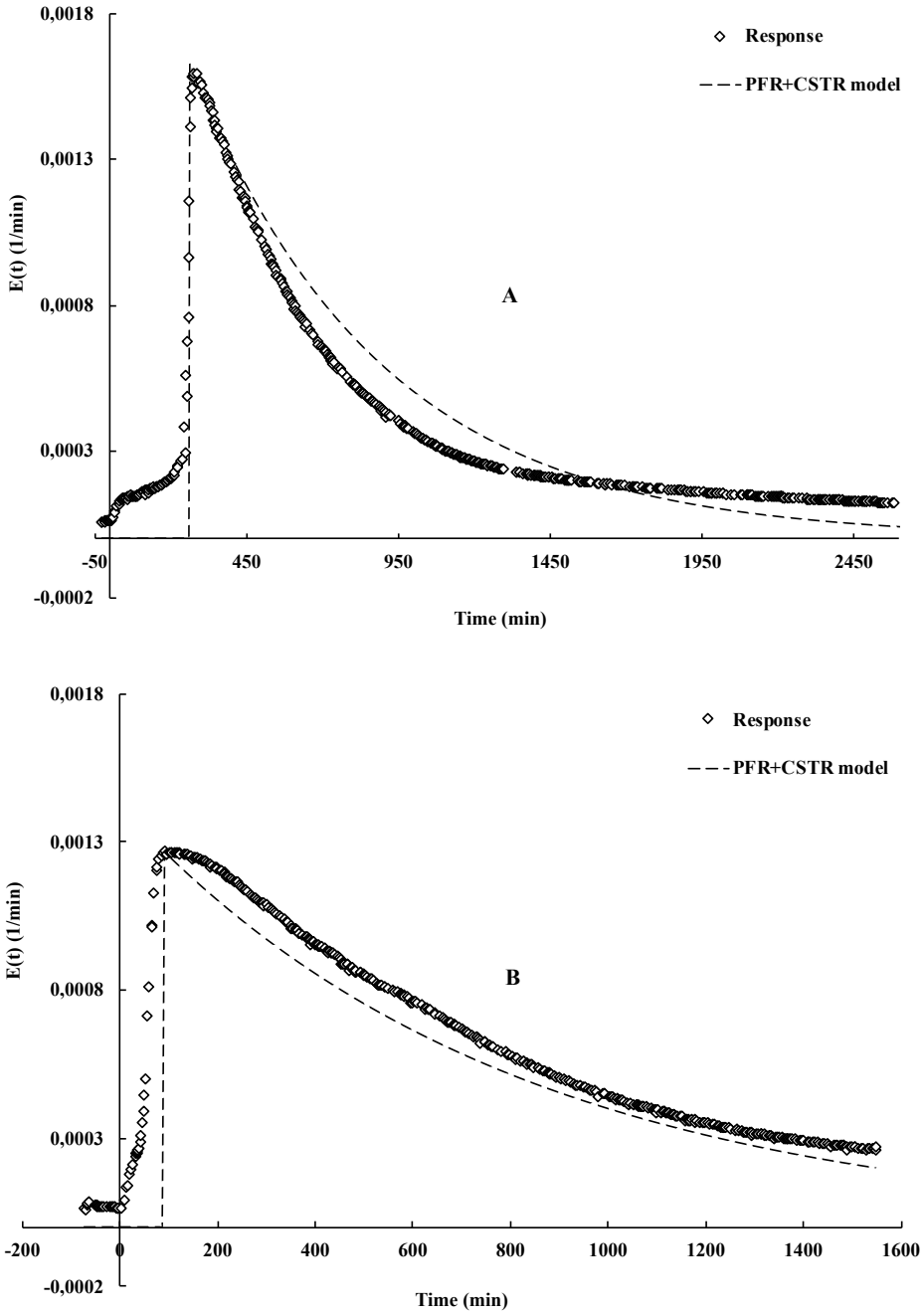

525 *Figure 2: RTD for the UASB reactor without (A) and with (B) a CSTR in recycle*

526

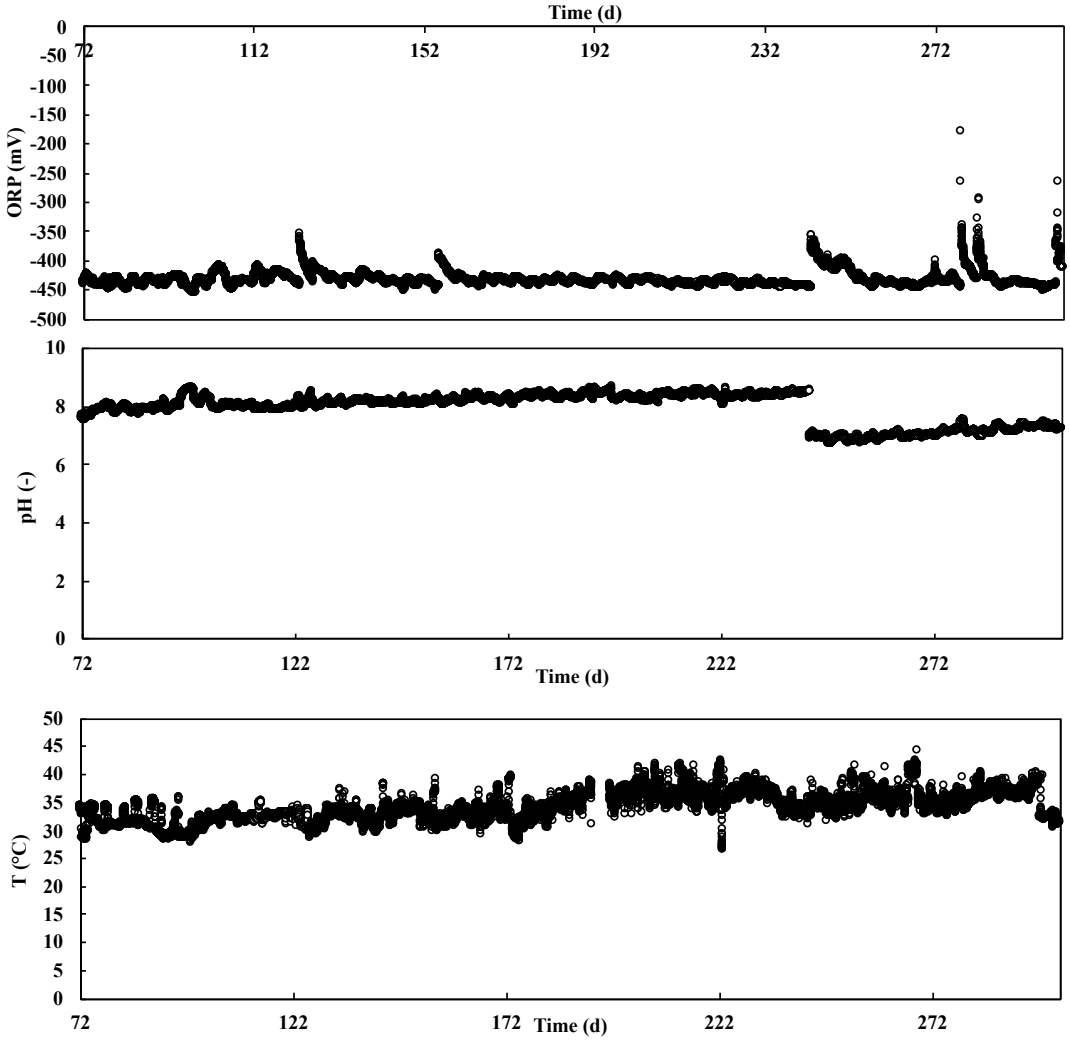

527

528 *Figure 3: ORP, pH and T values inside the UASB reactor*

529

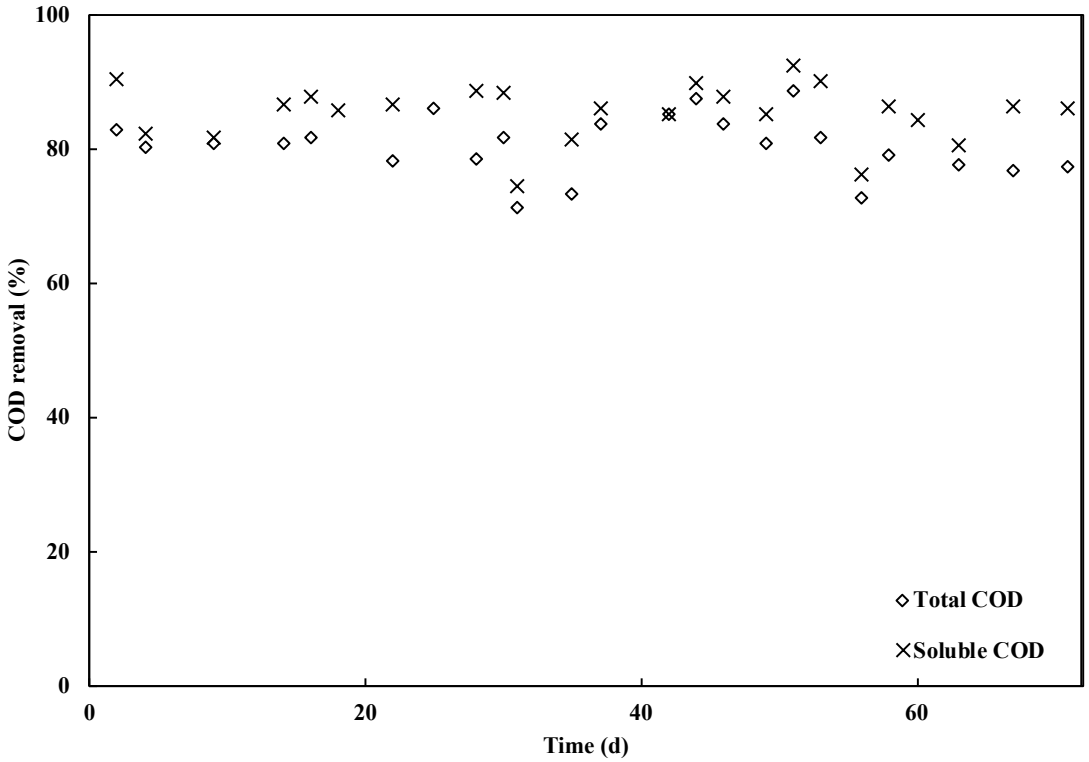

530

531 *Figure 4: Total and soluble COD removal efficiency for the UASB reactor during the*

532 *first experimental run*

533

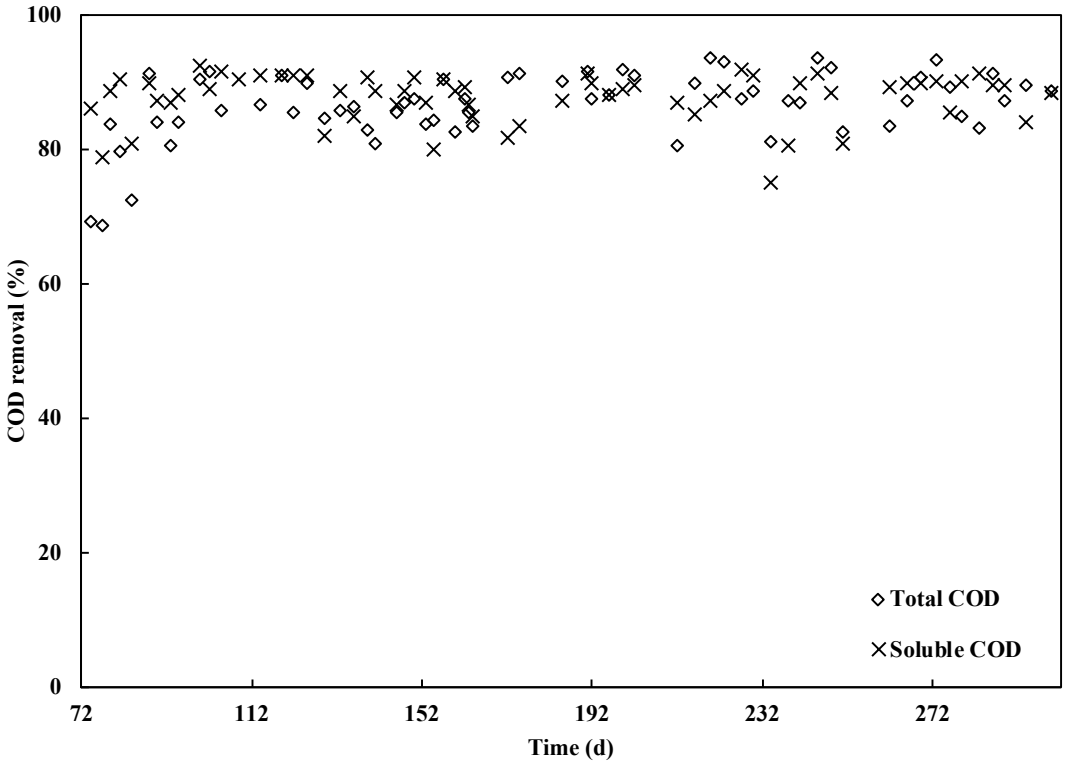

534

535 *Figure 5: Total and soluble COD removal efficiency for the UASB reactor with 1/1*

536 *recycle ratio during the second experimental run*

537

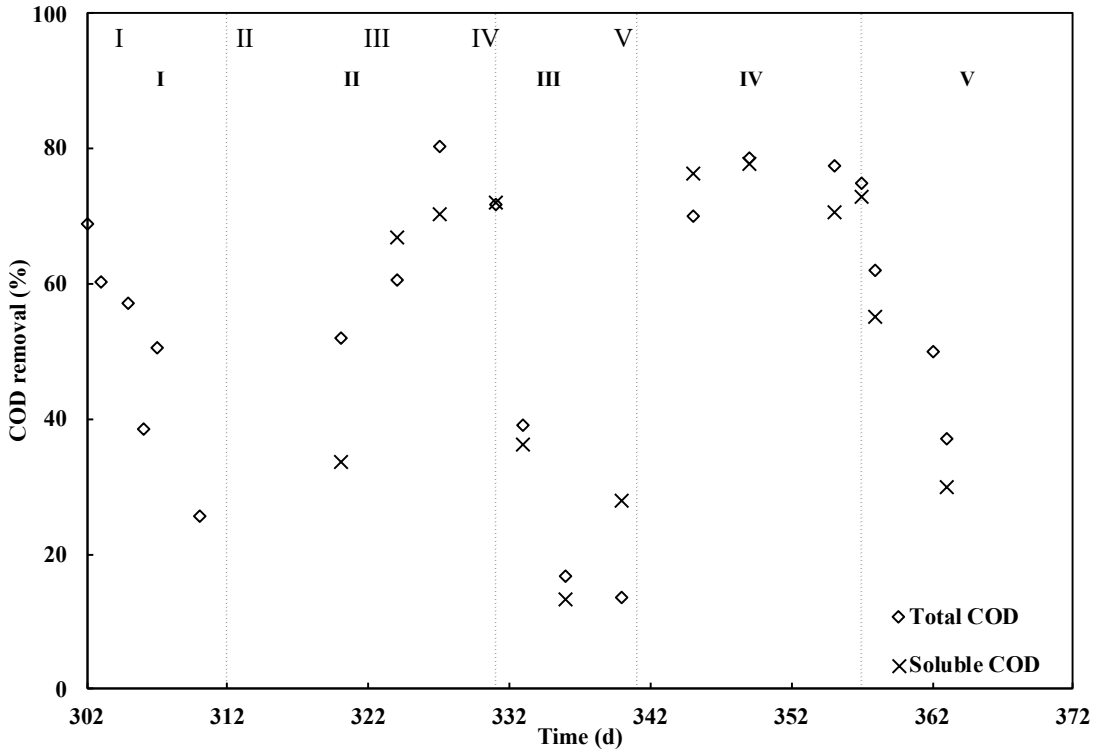

538

539 *Figure 6: Total and soluble COD removal efficiency for the UASB reactor with 1/1*

540 *recycle and eAOP treatment during the third experimental run*

541

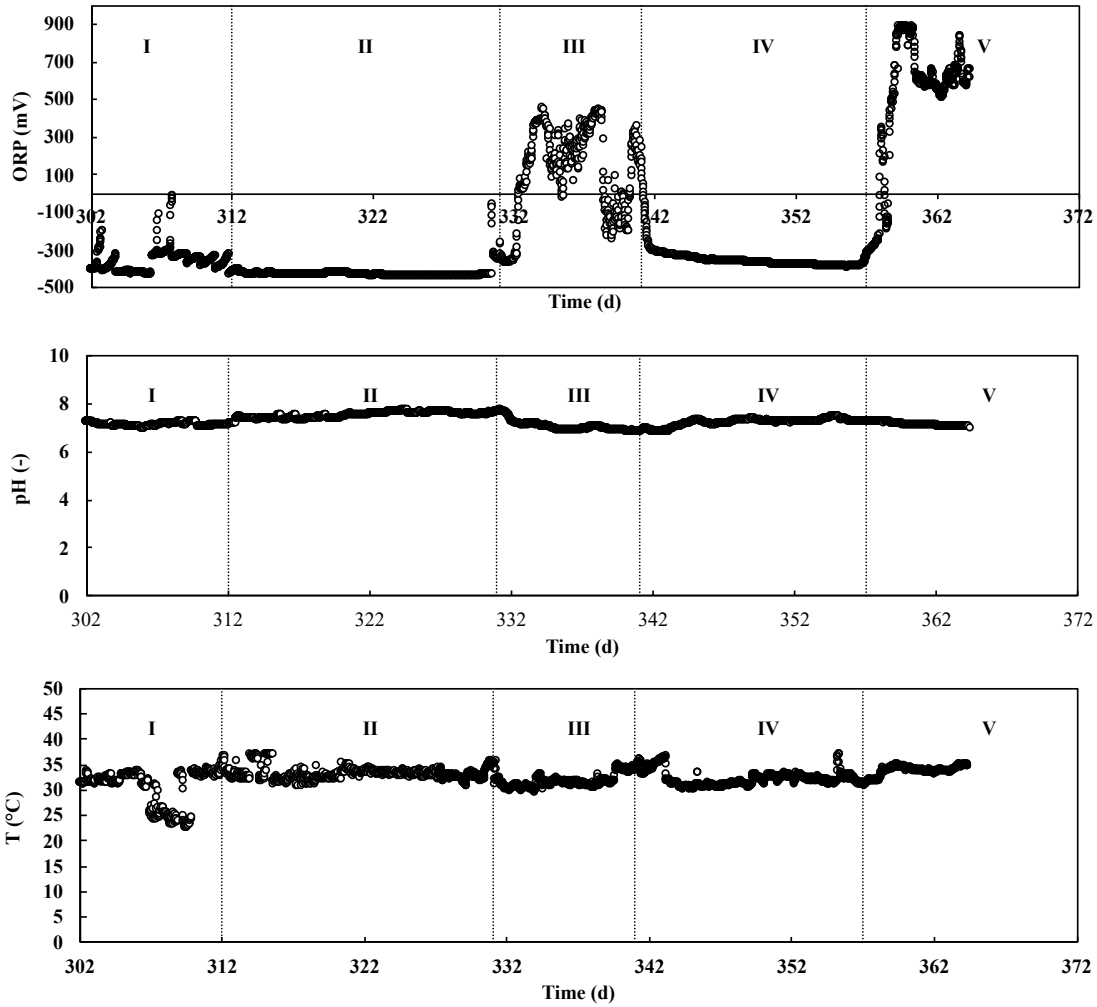

542

543 *Figure 7: ORP, pH and T values inside the UASB reactor treating 4-CP in recycle*

544 *during the third experimental run*

545